

Rabi oscillations under ultrafast excitation of graphene

P. N. Romanets and F. T. Vasko*

Institute of Semiconductor Physics, NAS of Ukraine, Pr. Nauky 41, Kiev 03028, Ukraine

(Received 27 April 2010; published 21 June 2010)

We study coherent nonlinear dynamics of carriers under ultrafast interband excitation of an intrinsic graphene. The Rabi oscillations of response appear with increasing of pumping intensity. The photoexcited distribution is calculated versus time and energy taking into account the effects of energy relaxation and dephasing. Spectral and temporal dependencies of the response on a probe radiation (transmission and reflection coefficients) are considered for different pumping intensities and the Rabi oscillations versus time and intensity are analyzed.

DOI: [10.1103/PhysRevB.81.241411](https://doi.org/10.1103/PhysRevB.81.241411)

PACS number(s): 78.47.jh, 78.67.Wj

The Rabi oscillations of coherent response under ultrafast excitation of two-level atomic systems were studied during last decades.¹ The similar phenomena in bulk semiconductors and quantum wells have also been observed under interband excitation, see Refs. 2 and 3 and reviews.^{4,5} In addition, the intersubband Rabi oscillations in quantum wells were studied in the mid-IR spectral region.⁶ Recently, the properties of graphene under ultrafast interband excitation were investigated, and most attention has been concentrated on relaxation dynamics for the case of the linear excitation regime of epitaxial and exfoliated graphene, see Refs. 7 and 8, respectively. It was found that the relaxation times of photoexcited electron-hole pairs due to the optical-phonon emission are about 0.1 ps.^{7,8} Therefore, an investigation of coherent dynamics is possible during the femtosecond time scales, when the regime of Rabi oscillations can be realized at strong enough pumping intensities. To the best of our knowledge, neither experimental nor theoretical treatment of the nonlinear coherent response for the Rabi oscillations regime in graphene is performed yet. Due to the gapless and massless energy spectrum with a neutrino-like dispersion law $\pm v_W p$ ($v_W \approx 10^8$ cm/s is the characteristic velocity for the Weyl-Wallace model⁹), such a case should be essentially different from the above-mentioned cases.²⁻⁵

In this Rapid Communication, we consider the nonlinear coherent process of carrier photoexcitation in an intrinsic graphene under the slow-envelope condition, $\Omega \tau_p \gg 1$, where Ω is the frequency of light and τ_p is the duration of excitation. Eliminating the nondiagonal components of density matrix, which are responsible for the high-frequency $[\propto \exp(-i\Omega t)]$ oscillations of polarization,¹⁰ we describe such a process by the same distribution functions for electrons and holes f_{pt} because of the electron-hole symmetry. The kinetic equation for f_{pt} takes form

$$\frac{df_{pt}}{dt} = G(f_p|t) + J_0(f_i|p), \quad (1)$$

where $G(f_p|t)$ is the interband generation rate and $J_0(f_i|p)$ is the collision integral. The general consideration of Eq. (1) can be found in Ref. 11 and the evaluation of the generation rate for graphene is performed in Ref. 12. Further, we solve this equation and analyze the spectral and temporal dependencies of the transmission and reflection coefficients for a probe radiation at different pumping levels.

The coherent interband photoexcitation caused by the in-plane electric field $w_t \mathbf{E} \exp(-i\Omega t) + \text{c.c.}$ with the envelope form factor w_t is described by the generation rate in Eq. (1) (Ref. 12),

$$G(f_p|t) = \left(\frac{eE v_W}{\hbar \Omega} \right)^2 w_t \int_{-\infty}^0 dt' w_{t+t'} e^{t'/\tau_d} \times \cos \left[\left(\frac{2v_W p}{\hbar} - \Omega \right) t' \right] (1 - 2f_{pt+t'}). \quad (2)$$

Here we neglect the multiphoton interband transitions under the condition $(eE v_W / \hbar \Omega^2)^2 \ll 1$ and the dephasing relaxation time τ_d is introduced phenomenologically. The nonlocal factor $(1 - 2f_{pt+t'})$ describes the population effect with the temporal memory which is responsible for the Rabi oscillations.¹⁰ Since the cascade emission of optical phonons dominates in the energy relaxation,^{7,8,13} Eq. (1) involves the collision integral

$$J_0(f_i|p) = \nu_{p+p_0} (1 - f_{pt}) f_{p+p_0t} - \nu_{p-p_0} (1 - f_{p-p_0t}) f_{pt}, \quad (3)$$

where $p_0 = \hbar \omega_0 / v_W$ is the characteristic momentum, $\hbar \omega_0$ is the optical-phonon energy, and $\nu_p = v_0 p / \hbar$ is the relaxation rate for the spontaneous emission of optical phonons. Under the condition $\nu_{p_0} \tau_p \ll 1$ we neglect interband transitions due to optical-phonon emission. We also restrict ourselves by the model with a single phonon of energy $\hbar \omega_0 \approx 0.2$ eV with the efficiency of coupling determined by the characteristic velocity $v_0 \approx 10^6$ cm/s. These parameters are in agreement with the results of calculations of the electron-phonon interaction¹⁴ and with the measurements of relaxation dynamics.^{7,8} The problem given by Eqs. (1)–(3) is solved below with the initial condition $f_{pt \rightarrow -\infty} = 0$ which is correspondent to the undoped graphene.

The analytical solution of the problem formulated here can be found for the collisionless case, $\tau_d \rightarrow \infty$ and $v_0 \rightarrow 0$, under the resonant condition $p \rightarrow \hbar \Omega / 2v_W \equiv p_\Omega$, when the oscillating factor is absent in the integral generation rate [Eq. (2)]. For such a case, the integrodifferential Eq. (1) can be transformed into the second-order differential equation and the solution takes form

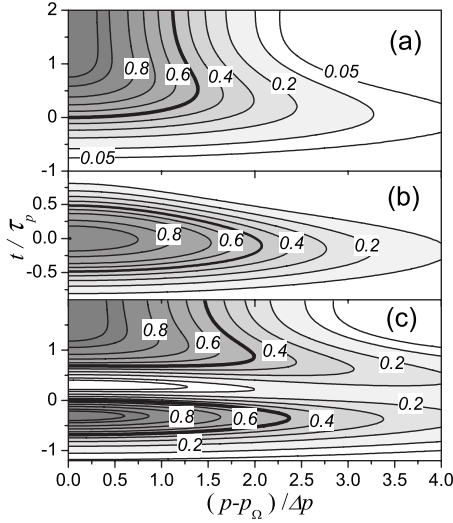


FIG. 1. Contour plots of photoexcited distribution $f_{p,t}$ versus dimensionless momentum and time, $(p-p_{\Omega})/\Delta p$ and t/τ_p for the collisionless regime at pumping levels corresponding to (a) $\mathcal{A}_{ex}=\pi$, (b) 2π , and (c) 3π .

$$f_{p=p_{\Omega},t} = \frac{1}{2} \left[1 - \cos \left(\sqrt{2I_{ex}} \int_{-\infty}^t \frac{dt'}{\tau_p} w_{t'} \right) \right]. \quad (4)$$

Here we introduced the dimensionless intensity, $I_{ex} = (eE\tau_p v_W / \hbar \Omega)^2$, so that the Rabi oscillations of the resonant distribution with time and with field strength ($\sqrt{2I_{ex}} \propto E$) takes place. At $t \rightarrow \infty$ one obtains the resonant distribution $f_{p=p_{\Omega},t \rightarrow \infty} = (1 - \cos \mathcal{A}_{ex})/2$ which is determined by the dimensionless area of the incident pulse $\mathcal{A}_{ex} = \sqrt{2I_{ex}} \int_{-\infty}^{\infty} dt w_t / \tau_p$.

The collisionless case at $p \neq p_{\Omega}$ is described by the reduced Eq. (1) $df_{p,t}/dt = G(f_p|t)$. The numerical solution of this equation is obtained here with the use of the finite-difference method¹⁵ and the Gaussian form factor $w_t = \sqrt{2/\pi} \exp[-(t/\tau_p)^2]$.¹⁶ In Fig. 1 we plot $f_{p,t}$ versus dimensionless time, t/τ_p , and momentum $(p-p_{\Omega})/\Delta p$ which is centered at p_{Ω} . Here $\Delta p = \hbar/(v_W \tau_p)$ determines a width of photoexcited distribution at $t \geq 2\tau_p$ while a width of distribu-

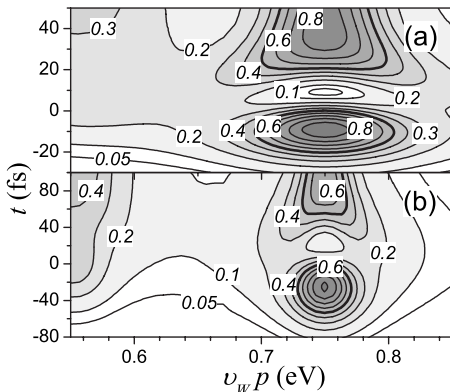


FIG. 2. Contour plots of photoexcited distributions $f_{p,t}$ versus energy v_{WP} and time for pulse durations (a) $\tau_p=30$ fs and (b) $\tau_p=80$ fs at pumping level corresponding to $\mathcal{A}_{ex}=3\pi$.

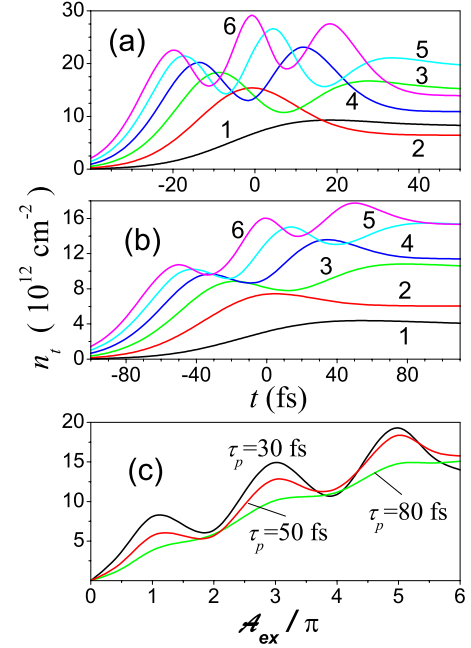


FIG. 3. (Color online) Transient evolution of concentration of photoexcited carriers for pulse durations (a) $\tau_p=30$ fs and (b) $\tau_p=80$ fs at pumping levels corresponding to (1) $\mathcal{A}_{ex}=\pi$, (2) $\mathcal{A}_{ex}=2\pi$, (3) $\mathcal{A}_{ex}=3\pi$, (4) $\mathcal{A}_{ex}=4\pi$, (5) $\mathcal{A}_{ex}=5\pi$, and (6) $\mathcal{A}_{ex}=6\pi$. (c) Photoexcited concentration versus \mathcal{A}_{ex} at $t \geq \tau_p$ for different τ_p (marked).

tion at $t=0$ increases with pumping intensity, as it is shown in Figs. 1(a)–1(c). As I_{ex} increases, a temporal Rabi oscillations at $p \neq p_{\Omega}$ became similar to the transient evolution described by Eq. (4).

We turn now to consideration of the problems (1)–(3) taking into account the dephasing and energy relaxation processes, when τ_d and v_0 are finite. In the calculations below we use the pumping frequency $\hbar\Omega=1.5$ eV and the dephasing time $\tau_d \approx v_{p_{\Omega}}^{-1}=85$ fs, which is correspondent to the process of spontaneous emission of optical phonons. Since the

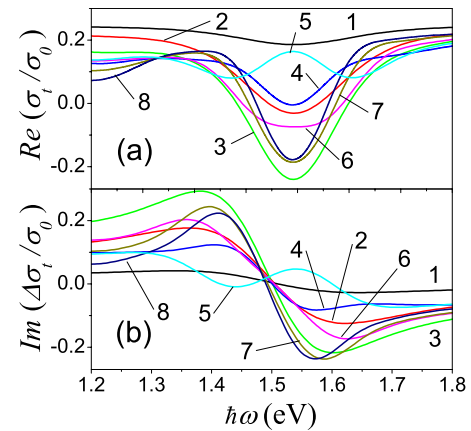


FIG. 4. (Color online) Spectral dependencies of the dynamic conductivity, (a) $\text{Re} \sigma_{\omega t}$ and (b) $\text{Im} \Delta \sigma_{\omega t}$, around the pumping energy 1.5 eV for delay times between -30 and 40 fs with step 10 fs (marked by 1–8) at pumping level corresponding to $\mathcal{A}_{ex}=3\pi$ and pulse duration $\tau_p=30$ fs.

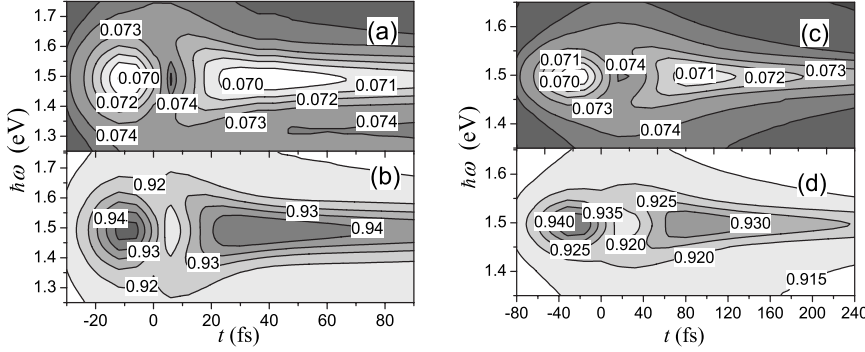


FIG. 5. Contour plots of reflection [(a) and (c)] and transmission [(b) and (d)] coefficients versus energy of probe radiation $\hbar\omega$ and time for pulse durations $\tau_p = 30$ fs [(a) and (b)] and 80 fs [(c) and (d)] at pumping level corresponding to $\mathcal{A}_{ex} = 3\pi$.

cascade emission of dispersionless optical phonons, described by Eq. (3), a multipeak structure of f_{pt} with maxima centered around $p_{\Omega} - kp_0$ ($k=0,1,\dots$) is realized. The only first phonon repetition is essential during the photoexcitation process, when $t \leq 2\tau_p$, see Figs. 2(a) and 2(b) where the contour plots of the photoexcited distributions f_{pt} at the pumping level $\mathcal{A}_{ex} = 3\pi$ are shown for the pulse durations $\tau_p = 30$ and 80 fs. One can see that the photoexcited distribution appears to be narrower with increasing of τ_p and that the Rabi oscillations are visible at $\tau_d \sim \tau_p$ [Fig. 2(b)].

Using the distribution f_{pt} obtained, we calculate here the concentration of photoexcited carriers

$$n_t = \frac{2}{\pi\hbar^2} \int_0^{\infty} dp p f_{pt} \quad (5)$$

versus time and versus pumping level at $t \gg \tau_p$. As one can see from Figs. 3(a) and 3(b), the amplitudes of temporal oscillations decreases with increasing of τ_p but the oscillations remain visible at $\tau_p \sim \tau_d$. The oscillatory behavior of $n_{t \rightarrow \infty}$ versus pumping level (which is proportional to \mathcal{A}_{ex}^2) appears to be suppressed at $\tau_p \sim \tau_d$ as it is shown in Fig. 3(c). The condition $\mathcal{A}_{ex} = \pi$ corresponds to the pulse energies ~ 15 or ~ 5.6 nJ for $\tau_p = 30$ or 80 fs and for the spot area $\sim 10^{-4}$ cm² (note, that the pulse energy $\propto \tau_p^{-1}$ and $\propto n^2$, if $\mathcal{A}_{ex} = n\pi$).

The transient response on a probe radiation $\propto \exp(-i\omega t)$ is determined by the dynamic conductivity $\sigma_{\omega t}$ which was evaluated in Refs. 11 and 17 for the collisionless case $\omega\tau_d \gg 1$, when the parametric dependency on time takes place. The real and imaginary parts of $\sigma_{\omega t}$ are given by

$$\begin{aligned} \text{Re } \sigma_{\omega t} &= \frac{e^2}{4\hbar} (1 - 2f_{p_{\omega t}}), \\ \text{Im } \sigma_{\omega t} &= \bar{\sigma}_{\omega} - \frac{e^2}{\pi\hbar} \mathcal{P} \int_0^{\infty} \frac{dy y^2}{1 - y^2} f_{p_{\omega y, t}}, \end{aligned} \quad (6)$$

where \mathcal{P} means the principle value of integral and we introduced the time-independent contribution $\bar{\sigma}_{\omega}$ described the undoped graphene in the absence of photoexcitation (below we use the phenomenological expression for $\bar{\sigma}_{\omega}$ introduced in Ref. 18). The negative absorption condition $\text{Re } \sigma_{\omega t} < 0$ takes place if $f_{p_{\omega t}} > 1/2$; these regions were marked by thick curves in Figs. 1 and 2. The peak shape of $\text{Re } \sigma_{\omega t}$ centered at $\omega = \Omega$ leads to a visible spectral dispersion of $\text{Im } \sigma_{\omega t}$ at $\omega < \Omega$ and $\omega > \Omega$, as shown in Fig. 4 where $\Delta\sigma_t = \sigma_{\omega t} - \bar{\sigma}_{\omega}$ and $\sigma_0 = e^2/\hbar$.

The reflection and transmission coefficients, $R_{\omega t}$ and $T_{\omega t}$, are written through the dynamic conductivity as follows:¹⁸

$$\begin{aligned} R_{\omega t} &= \left| \frac{1 - \sqrt{\epsilon} - 4\pi\sigma_{\omega t}/c}{1 + \sqrt{\epsilon} + 4\pi\sigma_{\omega t}/c} \right|^2, \\ T_{\omega t} &= \frac{4\sqrt{\epsilon}}{|1 + \sqrt{\epsilon} + 4\pi\sigma_{\omega t}/c|^2}. \end{aligned} \quad (7)$$

Here ϵ is the dielectric permittivity of a thick substrate and the geometry of normal propagation of radiation was considered. The contour plots of $R_{\omega t}$ and $T_{\omega t}$ versus t and ω are shown in Fig. 5 at pumping level corresponding to $\mathcal{A}_{ex} = 3\pi$ for $\tau_p = 30$ and 80 fs (Fig. 2). Temporal oscillations of response correlate with the evolution of $\sigma_{\omega t}$ (Fig. 4) due to oscillations of distribution shown in Fig. 2. Spectral width of Rabi oscillations appears to be broader for $\tau_p = 30$ fs [cf. Figs. 5(a)–5(d) with Figs. 2(a) and 2(b)]. The oscillatory behaviors of the reflection and transmission coefficients at the pumping frequency ($\omega = \Omega$), $R_{\Omega t}$, and $T_{\Omega t}$, versus pumping level for the delay times τ_p , $2\tau_p$, and $3\tau_p$ are shown in Figs. 6(a) and 6(b), respectively. One can see a few-percent modulation of response at $t \geq \tau_p$ versus pumping intensity. A visible damping of this modulation takes place due to the cascade emission of optical phonons, at $t \geq \nu_{p\Omega}^{-1}$.

Our calculations are based on the following assumptions. Since the Coulomb renormalization of interband transitions

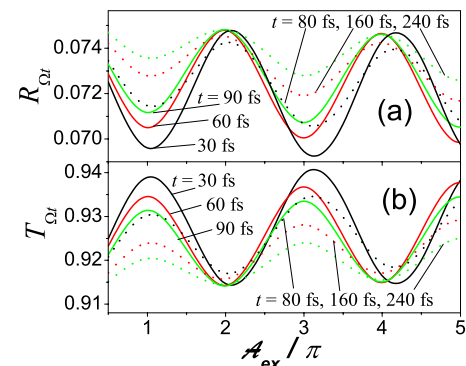


FIG. 6. (Color online) (a) Reflection and (b) transmission versus intensity for $\tau_p = 30$ and 80 fs (solid and dotted curves) at different delay times $t = \tau_p$, $2\tau_p$, and $3\tau_p$ (marked) and for $\omega = \Omega$.

is weak,¹⁹ we have used a single-particle approach. All homogeneous dephasing mechanisms, including optical-phonon emission and carrier-carrier scattering, have been described phenomenologically, through the dephasing time τ_d in Eq. (2). An inhomogeneous broadening due to long-scale disorder is not taken into account so that the results are valid for a high-quality graphene. The model collision integral [Eq. (3)], which is written through an effective phonon energy $\hbar\omega_0$ and a relaxation frequency ν_p , is used because the only first step of cascade emission of phonons is essential during the Rabi oscillation process. More exact calculations of Eq. (3) can improve a precision of ν_0 used and will give a widened peak of distribution at $p_\Omega - p_0$. The above-listed simplifications of the damping processes do not change the temporal dynamics under consideration and we have demonstrated that the Rabi oscillations are observable in a typical

graphene sample. The rest of assumptions [the geometry of normal propagation of radiation, the Gaussian shape of excitation, and the collisionless approximation used in Eq. (6)] are rather standard.

Summarizing, we have described the mechanisms of coherent nonlinear response of an intrinsic graphene under ultrafast interband excitation. The results obtained demonstrate that the Rabi oscillations, both versus time and versus pumping intensity, can be easily observed for femtosecond time scales (up to 0.1–0.2 ps) at pumping intensities $\sim 3\text{--}30\text{ GW/cm}^2$ (which are correspondent to pulse energies $\sim 10\text{--}100\text{ nJ}$ for the spot area $\sim 10^{-4}\text{ cm}^2$). The similar oscillations can be measured under mid-IR pumping, with $\hbar\Omega \sim 120\text{ meV}$,⁶ where the pulse duration can be up to $\sim 0.5\text{ ps}$ for a clean sample and the pumping intensities are $\sim 3\text{--}10\text{ MW/cm}^2$.

*ftvasko@yahoo.com

¹L. Allen and J. H. Eberly, *Optical Resonance and Two-Level Atoms* (Dover, NY, 1987); M. O. Scully and M. S. Zubairy, *Quantum Optics* (Cambridge University Press, Cambridge, 1997).

²H. Giessen, A. Knorr, S. Haas, S. W. Koch, S. Linden, J. Kuhl, M. Hetterich, M. Grun, and C. Klingshirn, *Phys. Rev. Lett.* **81**, 4260 (1998); C. Fürst, A. Leitenstorfer, A. Nutsch, G. Trankle, and A. Zrenner, *Phys. Status Solidi B* **204**, 20 (1997).

³A. Schülzgen, R. Binder, M. E. Donovan, M. Lindberg, K. Wundke, H. M. Gibbs, G. Khitrova, and N. Peyghambarian, *Phys. Rev. Lett.* **82**, 2346 (1999); S. T. Cundiff, A. Knorr, J. Feldmann, S. W. Koch, E. O. Gobel, and H. Nickel, *ibid.* **73**, 1178 (1994).

⁴F. Rossi and T. Kuhn, *Rev. Mod. Phys.* **74**, 895 (2002).

⁵V. M. Axt and T. Kuhn, *Rep. Prog. Phys.* **67**, 433 (2004).

⁶C. W. Luo, K. Reimann, M. Woerner, T. Elsaesser, R. Hey, and K. H. Ploog, *Phys. Rev. Lett.* **92**, 047402 (2004); T. Elsaesser and M. Woerner, *Phys. Rep.* **321**, 253 (1999).

⁷J. M. Dawlaty, S. Shivaraman, M. Chandrashekar, F. Rana, and M. G. Spencer, *Appl. Phys. Lett.* **92**, 042116 (2008); D. Sun, Z.-K. Wu, C. Divin, X. Li, C. Berger, W. A. de Heer, P. N. First, and T. B. Norris, *Phys. Rev. Lett.* **101**, 157402 (2008).

⁸R. W. Newson, J. Dean, B. Schmidt, and H. M. van Driel, *Opt. Express* **17**, 2326 (2009).

⁹E. M. Lifshitz, L. P. Pitaevskii, and V. B. Berestetskii, *Quantum Electrodynamics* (Butterworth-Heinemann, Oxford, 1982); P. R. Wallace, *Phys. Rev.* **71**, 622 (1947).

¹⁰Our consideration is based on the temporally nonlocal generation rate [Eq. (2)] and we do not use the semiconductor Bloch equations approach with the polarization $\propto \exp(-i\Omega t)$, see H. Haug and A.-P. Jauho, *Quantum Kinetics in Transport and Optics of Semiconductors* (Springer, Berlin, 1996) and Refs. 4 and 5.

¹¹F. T. Vasko and O. E. Raichev, *Quantum Kinetic Theory and Applications* (Springer, NY, 2005).

¹²P. N. Romanets and F. T. Vasko, *Phys. Rev. B* **81**, 085421 (2010).

¹³H. Wang, J. Strait, P. George, S. Shivaraman, V. Shields, M. Chandrashekar, J. Hwang, C. Ruizvargas, F. Rana, M. Spencer, and J. Park, *Appl. Phys. Lett.* **96**, 081917 (2010).

¹⁴H. Suzuura and T. Ando, *J. Phys. Soc. Jpn.* **77**, 044703 (2008); F. Rana, P. A. George, J. H. Strait, J. Dawlaty, S. Shivaraman, Mvs Chandrashekar, and M. G. Spencer, *Phys. Rev. B* **79**, 115447 (2009).

¹⁵D. Potter, *Computational Physics* (Wiley, London, 1973).

¹⁶The form factor w_l is normalized as $\int_{-\infty}^{\infty} dt w_l^2 = \tau_p$. The shape of w_l has little effect on the photoexcitation process because the response is mainly dependent on τ_p .

¹⁷L. A. Falkovsky, *Phys. Usp.* **51**, 887 (2008); T. Stauber, N. M. R. Peres, and A. K. Geim, *Phys. Rev. B* **78**, 085432 (2008).

¹⁸M. V. Strikha and F. T. Vasko, *Phys. Rev. B* **81**, 115413 (2010); M. Bruna and S. Borini, *Appl. Phys. Lett.* **94**, 031901 (2009).

¹⁹D. E. Sheehy and J. Schmalian, *Phys. Rev. B* **80**, 193411 (2009); L. Yang, J. Deslippe, C.-H. Park, M. L. Cohen, and S. G. Louie, *Phys. Rev. Lett.* **103**, 186802 (2009).